



LAWRENCE  
LIVERMORE  
NATIONAL  
LABORATORY

# An ab initio Molecular Dynamics study of the solvated OHCl<sup>-</sup> complex. Implications for the atmospheric oxidation of (Cl<sup>-</sup>)<sub>aq</sub> to (Cl<sub>2</sub>)<sub>g</sub>

R. D'Auria, I-F. W. Kuo, D. J. Tobias

August 3, 2007

Journal of Physical Chemistry A

## **Disclaimer**

---

This document was prepared as an account of work sponsored by an agency of the United States government. Neither the United States government nor Lawrence Livermore National Security, LLC, nor any of their employees makes any warranty, expressed or implied, or assumes any legal liability or responsibility for the accuracy, completeness, or usefulness of any information, apparatus, product, or process disclosed, or represents that its use would not infringe privately owned rights. Reference herein to any specific commercial product, process, or service by trade name, trademark, manufacturer, or otherwise does not necessarily constitute or imply its endorsement, recommendation, or favoring by the United States government or Lawrence Livermore National Security, LLC. The views and opinions of authors expressed herein do not necessarily state or reflect those of the United States government or Lawrence Livermore National Security, LLC, and shall not be used for advertising or product endorsement purposes.

**An *ab initio* Molecular Dynamics study of the solvated  $\text{OHCl}^-$  complex. Implications for the atmospheric oxidation of  $(\text{Cl}^-)_{aq}$  to  $(\text{Cl}_2)_g$**

**Raffaella D’Auria,<sup>\*</sup> I-F. William Kuo,<sup>†</sup> and Douglas J. Tobias<sup>‡</sup>**

Department of Chemistry and AirUCI, University of California, Irvine, Irvine, California 92697-2025; Computational Chemical Biology, Lawrence Livermore National Laboratory, P.O. Box 808, Livermore, California 94551.

rdauria@uci.edu, kuo2@llnl.gov, dtobias@uci.edu

**ABSTRACT**

We have studied the  $\text{OHCl}^-$  complex in a six water cluster and in bulk liquid water by means of generalized gradient-corrected BLYP density functional theory based Born-Oppenheimer molecular dynamics. Self-interaction corrected results, that predict an H-bonded  $\text{OH} \cdots \text{Cl}^-$  complex, are compared to the uncorrected ones, that predict a bonded  $(\text{HO}-\text{Cl})^-$ . A second order Møller-Plesset potential energy landscape of the gas-phase complex in its ground state was computed to determine which of the two configurations represents the true nature of the bond. Since no evidence of a local minimum was found in the vicinity of the geometry corresponding to the  $(\text{HO}-\text{Cl})^-$  we conclude that the complex is held together by a H-bond like interaction in both an asymmetric solvation environment, as represented by the cluster, and in a symmetric solvation environment, as represented by the bulk system. In the limits of the present results we

---

<sup>\*</sup>Department of Chemistry and AirUCI, University of California, Irvine.

<sup>†</sup>Computational Chemical Biology, Lawrence Livermore National Laboratory.

<sup>‡</sup>Department of Chemistry and AirUCI, University of California, Irvine.

postulate that the mechanism that governs the atmospheric oxidation of  $(\text{Cl}^-)_{int}$  to  $(\text{Cl}_2)_{gas}$  on the surface of marine aerosols [Knipping et al. 2000] is initiated by the formation of an H-bonded  $\text{OH}\cdots\text{Cl}^-$  complex. Furthermore, since no evidence of charge transfer mechanism from  $\text{Cl}^-$  to  $\text{OH}$  was found, in the liquid as well as in the cluster environments, a likely second step toward the oxidation of  $\text{Cl}^-$  should consist in the reaction of the complex with a second  $\text{Cl}^-$  that would result in the formation of the species  $\text{Cl}_2^-$  and  $\text{OH}^-$ .  $(\text{Cl}_2)_g$  could then be formed upon charge exchange reaction with an impinging  $\text{OH}$  molecule.

KEYWORDS

## Introduction

The interaction of chloride anion with water and  $\dot{\text{O}}\text{H}$  has been the subject of several experimental<sup>(1-3)</sup> as well as theoretical<sup>(3)</sup> investigations. Jayson *et al.*<sup>(1)</sup> conducted a series of pulse radiolysis experiments of aqueous sodium chloride solutions and interpreted their results on the basis of the following equilibria:



where the equilibria (1) and (2) are over to the left at low  $\text{Cl}^-$  concentration and at low acidity levels respectively. Operating at low acidity and high chloride concentration Jayson and coworkers

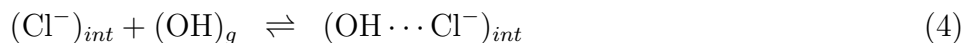
collected a spectra peaked at 350 nm which they attributed to a  $\text{ClOH}^-$  species.

Sevilla *et al.*<sup>(3)</sup> collected electron spin resonance (ESR) spectra after  $\gamma$ -irradiation of a series of frozen aqueous solutions containing  $\text{Cl}^-$ . Upon annealing of the samples from 77 K to up to 125 K they consistently detected a “stepwise development of the ESR signal of a  $\dot{\text{Cl}}\text{-X}$  species” accompanied by a decrease in the  $\dot{\text{O}}\text{H}$  signal. Sevilla and coworker attributed the observed ESR  $\dot{\text{Cl}}\text{-X}$  signal to the  $\dot{\text{Cl}} - \text{OH}_2$  complex rather than the  $\dot{\text{Cl}} - \text{OH}^-$  species since their experiments were run under low pH conditions. They pointed out, however, that the intermediate complex, formed as a result of the attack of the hydroxyl radical on the chloride anion, should be a chloride-hydroxy complex. A companion theoretical investigation of the interaction of chloride ions and hydroxyl radicals as well as the interaction between the chlorine atom and water was carried out in the Seviell *et al.* study. At the different level of theory employed in the computations (including uMP2/6-31+G\* and PM3) the authors noted that the equilibrium structure for the gas phase chloride ion-hydroxyl radical complex (with and without water) always has the hydrogen oriented toward the  $\text{Cl}^-$ . While the chlorine atom-water complexes are characterized by a three-electron hemibond between the unpaired electron in atomic chlorine and one lone pair of the water.

The  $\text{OHCl}^-$  complex has also been studied in the gas phase by Neumark and coworkers<sup>(4)</sup>. In this work a comparison of measured and computed photodetachment spectra of  $\text{OHCl}^-$  is presented. The complex structure was determined to be linear  $\text{OH} \cdots \text{Cl}^-$ .

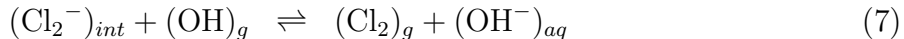
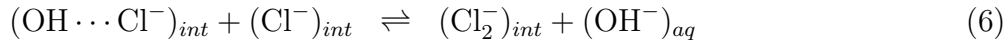
The wealth of work quickly reviewed above suggests that the chemistry of chloride ions and OH radiacals in an aqueous environment (as well as in the gas phase) is an intriguing problem which investigation poses challenges from the computational as well as the experimental point of view. In atmospheric chemistry, the interactions between the two species are eventually responsible for the oxidation of chloride ions present, for example, in marine aerosol, to gaseous

Cl<sub>2</sub> which, in urban environments, is a precursor of ozone, a dangerous tropospheric pollutant. Therefore a sound understanding of the fundamental chemistry beyond this oxidation process can help understand and predict the fate of tropospheric O<sub>3</sub>. In particular, marine aerosols, present in coastal regions, have been found to be a source of atmospheric molecular chlorine in the presence of an airborne oxidative species (such as OH)<sup>(5)</sup>. Heterogeneous chemistry has been invoked to explain the molecular chlorine yields observed in an aerosol chamber study<sup>(6)</sup>. A series of classical molecular dynamics studies have shown that a substantial population of chloride anion is found at the particle interface<sup>(7)</sup> and that OH accumulates at the air-particle interface<sup>(8)</sup>, thus making the formation of a OH⋯Cl<sup>-</sup> collisional complex possible. The proposed mechanism<sup>(6)</sup> for the oxidation of adsorbed Cl<sup>-</sup> at the particle interface to gaseous Cl<sub>2</sub> goes through the following steps:



The first step of this mechanism, reaction (4), requires the formation of a OH⋯Cl<sup>-</sup> complex as a result of the interaction between gaseous OH radicals impinging on the aerosol interface and an interfacial chloride anion. Roeselova et al. have computed the expected interfacial OH concentration to be around  $2.3 \times 10^{10}$  [radicals/cm<sup>3</sup>]<sup>(8)</sup>. Considering a coarse marine aerosol particle of 1 μm radius the number of OH radicals on such a particle would then be circa 0.1 radicals. This observation suggests that the number of such complexes at the interface should be low so that the second step of the oxidation mechanism, Reaction (5), could be expected to

be not very efficient. In the light of this observation Reaction (5) could be replaced by:



A possible alternative to the proposed mechanism, reactions (4) and (5), could be represented,



Reaction (8) is energetically uphill in the gas phase (since the electron affinity of Cl is  $\approx 1.78$  eV larger than the one of  $\text{OH}^{(9,10)}$ ). To understand whether in the presence of solvent the energetics become favorable for a charge transfer (i.e., reaction (8)) or if the chloride-hydroxy complex forms (i.e., reaction (4)), we have performed a series of ab initio molecular dynamics simulations on two analogous systems: a 6 waters  $\text{Cl}^- \cdots \text{H}\ddot{\text{O}}$  cluster and a bulk-like system containing 57 water molecules, one  $\text{Cl}^-$  and one  $\ddot{\text{O}}\text{H}$  with three dimensional periodic boundary conditions. The first system was designed to mimic an asymmetric solvation, environment such as an interface, while the second was devised to understand the role of a symmetric solvation environment. We have found that the oxidation mechanism does go through the formation of a chloride-hydroxy complex and that henceforth reaction (4) does occur in place of reaction (8). We have also found that for this class of open shell system particular care has to be taken when using DFT realization of ab initio molecular dynamics, as in the current study, to ensure that self interaction error is well

accounted for.

## Computational details

Ab initio molecular dynamics simulations were carried out for a representative cluster and bulk system up to 10.0 ps with a timestep of 0.48 fs. The cluster simulations, were performed in the micro-canonical (NVE) ensemble while the bulk simulations were performed in the canonical ensemble (NVT) using one Nose-Hoover thermostats for every degree of freedom and a characteristic frequency of  $2000\text{ cm}^{-1}$ . The interaction potential adopted is based on Kohn-Sham formulation of density functional theory as implemented in the simulation package CP2K<sup>(11)</sup>. The electronic structure was explicitly quench at everytime step to a tolerance of  $1.0\text{E-}7$  to conserve energy.

The electronic structure was computed via the QuickStep module in the simulation package CP2K<sup>(11,12)</sup>. The QuickStep module uses a dual basis set formalism of Gaussian type orbitals (TZV2P) and plane-waves expanded up to 280 Ry cutoff for the density<sup>(13)</sup>. With the use of plane-waves, the GTH<sup>(19)</sup> pseudopotential was employed to describe the core electronic states. The exchange and correlation energies are described using the BLYP functionals<sup>(20)</sup>. All calculation were carried out within the local spin density approximation. For comparison, we have performed all simulations with and without the self interaction correction scheme implemented by d’Avezac et al.<sup>(14)</sup> and implemented in CP2K by VandeVondele and Sprik<sup>(15)</sup>.

A single point uMP2/aug-cc-pVDZ computation was implemented for the 6 water cluster system in the HOCl<sup>-</sup> configuration to detect the presence of bonding orbitals. Also a potential energy surface (PES) scan was computed for the gas phase OHCl<sup>-</sup> complex at the same level of theory to understand whether the energy of the HOCl<sup>-</sup> is a local minimum on such PES.

The scan was performed varying the Cl-O distance and the Cl-O-H angle while keeping the OH distance fixed at 1 Å.

## Results and Discussion

Two sets of ab initio molecular dynamics simulations, one uncorrected for the self interaction error and the other corrected, were computed on two different systems: a  $(\text{HO}-\text{Cl})^-$  and 57 waters in a square box with 3-D periodic boundary conditions imposed, and a  $(\text{HO}-\text{Cl})^-\cdot(\text{H}_2\text{O})_6$  aggregate with cluster boundary conditions. In the following results from the two different systems are compared and the effect that the self interaction correction plays on the preferred structure geometry is discussed.

### $(\text{HO}-\text{Cl})^-$ versus H-bonded $\text{OH}\cdots\text{Cl}^-$

Two main chloride anion-hydroxyl radical complex structures have been identified in the simulations. In the standard DFT simulations, when SIE correction it is not considered, the complex appears in a  $(\text{ClOH})^-$  configuration. Analysis of its structure in terms of its geometry and by location of the WFCs (*vide infra*) indicates that in the cluster, as well as in the bulk case, the complex is held together by a Cl-O bond, this bond is likely to be a three electron kind of bond (hemibond) between the partially occupied oxygen orbital and one lone pair of the chloride ion (although we have not computed the Wannier orbitals and therefore we can only guess the true nature of the bond). In the SIE corrected DFT simulations the complex is found for the most part in a linear  $\text{OHCl}^-$  configuration and is therefore H-bonded. In Figure 1 the histograms of the Cl-O distance and the Cl-O-H angle are shown for the cluster simulations with no SIC (left panel) and with SIC (right panel). In the case when no SIC is considered the Cl-O-H angle

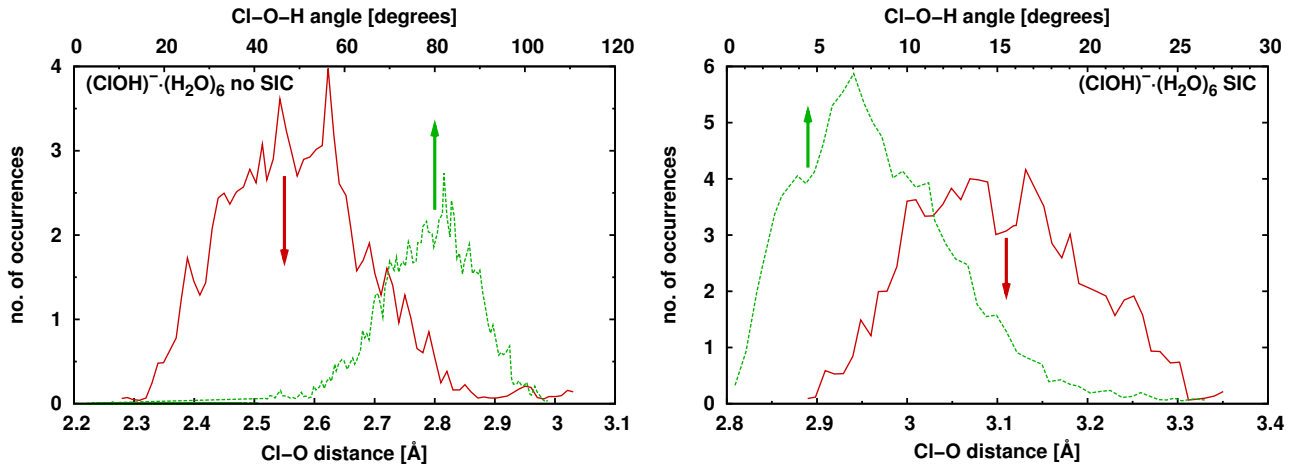


**Figure 1.** Histograms of the Cl–O distance and the Cl–O–H angle for the  $\text{Cl}^- \cdots \text{H}\ddot{\text{O}}$  complex in a six water cluster obtained from simulations with no SIC (left) and with SIC (right).

ranges around  $80^\circ$  and the histogram of the Cl–O distance has a peak around  $2.5 \text{ \AA}$ , while when the SIC is considered the histogram of the Cl–O–H angle peaks around  $7^\circ$  and the Cl–O most probable distance lays around  $3 \text{ \AA}$ .

In Figure 2 snapshots of the 6 water cluster DFT and SIC-DFT simulations are shown. In Figure 3 analogous snapshots are shown for the bulk simulations. In the snapshots the atoms are shown together with the centers of their maximally localized Wannier functions<sup>(16)</sup>. The maximally localized Wannier functions are analogous to localized molecular orbitals. They are obtained by transformation of the original delocalized Kohn-Sham orbitals. The position of the centers of such functions represents the maximum probability of finding an electron in such a place<sup>(17)</sup>. Within this interpretation of the Wannier function centers (WFCs) we can monitor the position where the negative charge is likely to be found. In the case of the standard DFT results, showed in the left panels of Figure 2 and Figure 3, the position of maximum probability for the extra electron appears to be in between the chlorine atom and the hydroxy, in line with what could be expected for a hemibond-like interaction. In the SIC corrected simulations the negative

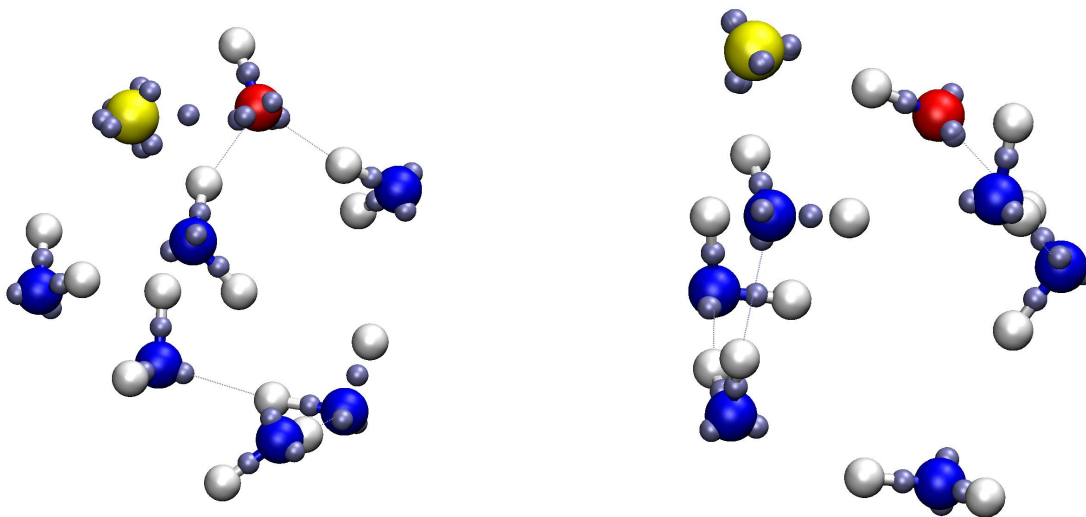


**Figure 2.** Hemibonded  $(\text{ClOH})^- \cdot (\text{H}_2\text{O})_6$ , left, versus H-bonded  $\text{OHCl}^- \cdot (\text{H}_2\text{O})_6$ , right, cluster geometries. Water oxygens are depicted in blue, while the OH oxygen is depicted in red, all the hydrogens are in white, the Cl atom is depicted in yellow, the gray spheres represents the Wannier function centers (WFCs) for the two systems (see text).

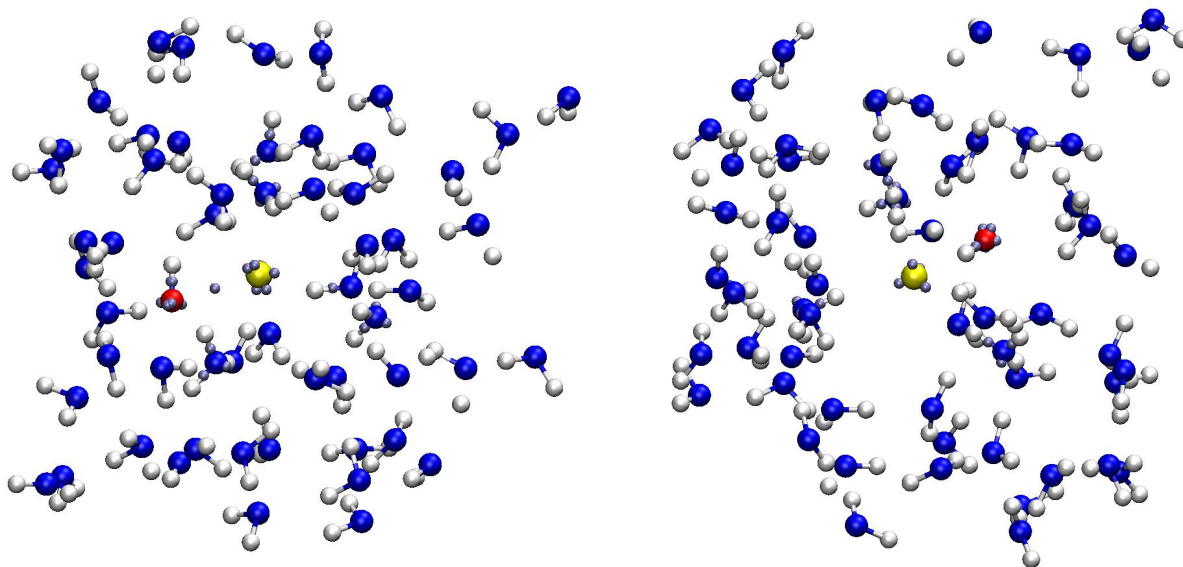


**Figure 3.** Hemibonded  $(\text{ClOH})^- \cdot (\text{H}_2\text{O})_6$ , left, versus H-bonded  $\text{OHCl}^- \cdot (\text{H}_2\text{O})_6$ , right, bulk geometries. Only the WFCs within 4 Å of the chlorine are shown. The atoms have the same coloring scheme as in Figure 2.

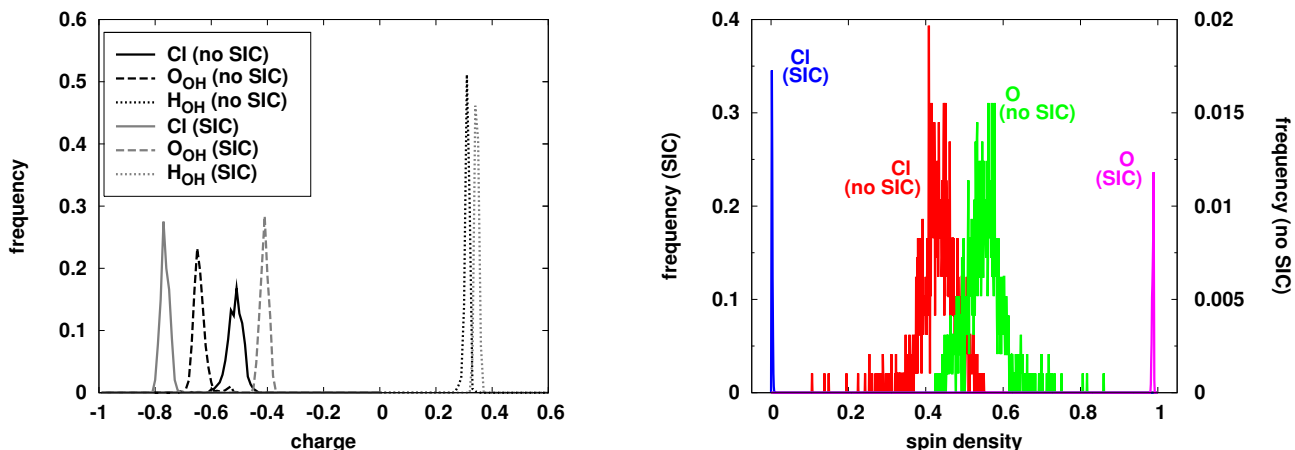


**Figure 4.** Histograms of the charge (left panel) and spin density (right panel) distributions obtained by a Mulliken analysis performed on the standard DFT and SIC-DFT six water cluster trajectories. In the standard DFT case the charge and the spin densities are largely shared between the oxygen of the radical and the chlorine atom. When DFT is corrected for SIE the net excess charge is largely concentrated on the chlorine while the spin density is mostly concentrated on the oxygen.

charge appears to be localized on the chlorine atom. In the simulations with no SIC the average distance between the shared WFC and the chlorine and the average distance between the shared WFC and the hydroxyl radical are of 1 Å.

To further characterize the nature of the two observed complexes we have performed a Mulliken analysis on the six water cluster DFT and SIC-DFT simulations to understand how the charge and the spin are partitioned in the two cases. In the covalently bonded structure the excess negative charge is roughly equally split between the Cl and the O atoms, concurrently the density of spin is smeared among the two species in accordance with what could be expected of a hemibond-like interaction. In the SIC-DFT results, where the complex is H-bonded, the excess charge is mostly centered on the chlorine while the spin is concentrated on the oxygen thus describing a  $\dot{\text{O}}\text{H}\cdots\text{Cl}^-$  complex.

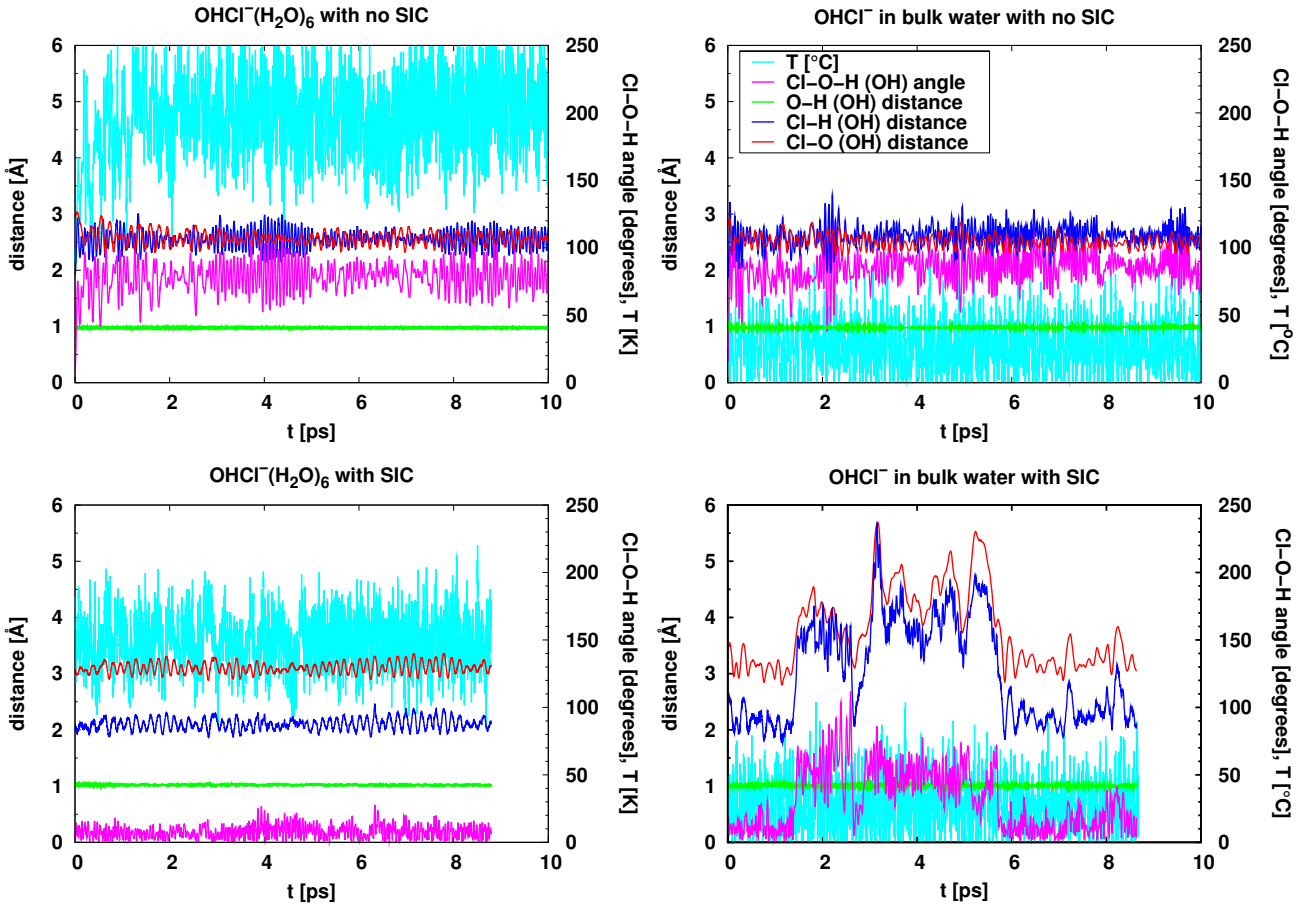


**Figure 5.** Time behavior of the geometrical factors characterizing the complex (*i.e.*, Cl-O distance, O-H distance, Cl-H distance, and Cl-O-H angle).

### Stability of the $\text{Cl}^- \cdots \text{H}\ddot{\text{O}}$ complex

To determine whether the OH and  $\text{Cl}^-$  were complexed throughout the simulation we have plotted the various internal distances of the complex, that is Cl-O, O-H, and Cl-H and the Cl-O-H angle as a function of time, the result is displayed in Figure 5. The trajectories for the bulk simulations are run in the NVT ensemble at room temperature, while the simulations of the six water cluster are run in the NVE ensemble. The average temperature of the cluster SIC-DFT is  $\sim 150$  K, while the temperature for the simulation with no SIC is  $\sim 200$  K. The results for the DFT and DFT-SIC simulations of the complex in the six water clusters, displayed

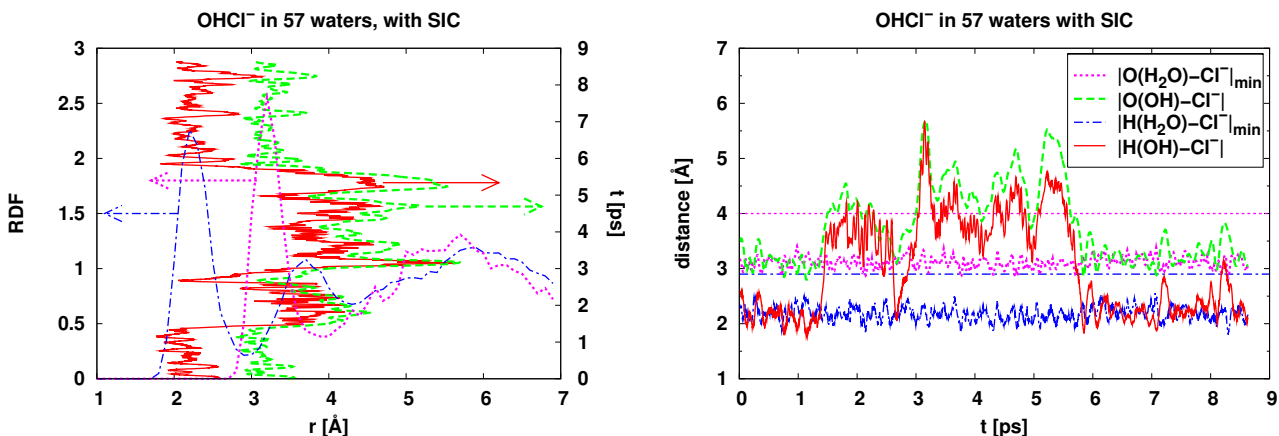


**Figure 6.** Left panel: Radial distribution functions of  $\text{H}_2\text{O}$  (blue line) and  $\text{O}_{\text{H}_2\text{O}}$  (purple line) about  $\text{Cl}^-$ . Overlaid to the RDFs are the values of the  $\text{Cl}-\text{O}_{\text{OH}}$  and  $\text{Cl}-\text{H}_{\text{OH}}$  distances as a function of time (green and red line respectively). Right panel:  $\text{Cl}-\text{H}_{\text{OH}}$  and  $\text{Cl}-\text{O}_{\text{OH}}$  distances as a function of time (red and green line respectively) and minima of the  $\text{Cl}-\text{O}_{\text{H}_2\text{O}}$  and  $\text{Cl}-\text{H}_{\text{H}_2\text{O}}$  distances (purple and blue line respectively). The purple horizontal line represents the location of the first minimum in the RDF of the water oxygens around chloride while the blue horizontal line represents the location of the first minimum in the RDF of the water hydrogens about the chloride ion (i.e., the radii of the respective first solvation shells).

on the left top and bottom panels of Figure 5 respectively, show that the complex is fairly stable.

The complex is also stable in the standard DFT bulk simulation, shown on the top left panel of Figure 5. In the SIE corrected simulation of  $\text{ClOH}^-$  in 57 water (with PBC), shown in the bottom right panel of Figure 5, the complex appear to break and re-form on the timescale of picoseconds. To understand the solvation dynamics in the latter case we have plotted in Figure 6 the  $\text{Cl}-\text{O}_{\text{OH}}$  and the  $\text{Cl}-\text{H}_{\text{OH}}$  distances with respect of the radial distribution function of the water oxygens and the water hydrogens about  $\text{Cl}^-$  (left panel) and with respect of the minimum distances of water oxygens and hydrogens to the chloride ion (right panel). On the timescale of our simulation the hydroxyl radical is always contained well within the water second solvation shell about the chloride ion. Although this feature could be due to the size of the fundamental simulation box ( $13\text{\AA} \times 13\text{\AA} \times 13\text{\AA}$ ), that does not extend beyond the water second solvation shell

about the ion, the chloride to hydroxy distance is never observed to become larger than the maximum in the chloride-water second solvation shell. Incidentally, the size of the period box resembles the situation in a concentrated solution in which another chloride ion would be found in the vicinity of the first, however in our simulation there is no counter ion.

It should be noted that the results of the Mulliken analysis for how regards the charge of the cluster system do not show a tendency of the system to undergo a charge exchange. Therefore we conclude that, given the degree of stability observed for the chloride-hydroxy complex in all four cases considered, and the localization of the charge in the two cluster system considered (with inclusion of SIE correction or not), Reaction (8) does not occur and the first step of the OH induced oxidation mechanism of the  $\text{Cl}^-$  start with the formation of the chloride-hydroxy complex through Reaction (4).

## Comparison with *ab initio* calculations

A single point uMP2/aug-cc-pVDZ computation of the covalently bonded six water cluster was performed to see whether a bonding molecular orbital could be detected. The cluster geometry on which the computation was performed was obtained by a snapshot of the corresponding molecular dynamics simulation. A bonding orbital was found and is displayed in Figure 7. All the computations presented in this section have been carried out using the Gaussian 98<sup>(18)</sup> suite of programs.

To understand the nature of the  $\text{OHCl}^-$  complex in the gas phase we have performed a uMP2/aug-cc-pVDZ scan of the potential energy surface varying the Cl-O-H angle and the Cl-O distance. The resulting potential energy landscape is reported in Figure 8. The scan was obtained keeping the OH distance fixed at  $1\text{\AA}$  while varying the Cl-O distance and the Cl-O-H

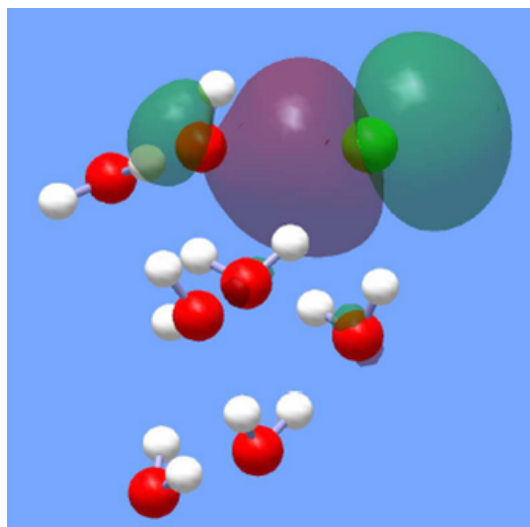


**Figure 7.** Bonding molecular orbital for the covalently bonded  $\text{OHCl}^-(\text{H}_2\text{O})_6$  cluster obtained from a single point uMP2/aug-cc-pVDZ computation.

angle. The covalently bonded structure observed in the SIE uncorrected DFT simulations of the complex in a six water cluster and in bulk water corresponds to a point on the PES of the gas phase complex ( $\text{Cl-O}=2.5\text{\AA}$  and  $\text{Cl-O-H}=78^\circ$ ) where no minimum is present. In Figure 9 we present a comparison of the PES scan for  $\text{O-H}=1\text{\AA}$  and  $\text{Cl-O-H}=0^\circ$  and  $78^\circ$  for the gas phase complex obtained with uMP2/aug-cc-pVDZ and with the standard BLYP and with SIC-BLYP. While both DFT computations for the linear  $\text{OHCl}^-$  complex show a minimum for a Cl-O distance of approximately  $=3.2\text{\AA}$  in agreement with the uMP2/aug-cc-pVDZ computation (albeit overestimating the binding energy), the results for the non linear structure (Cl-O-H angle of  $78^\circ$ ) show that the SIE-uncorrected DFT computation strongly overestimates the minimum around  $2.6\text{\AA}$  (note that the PES shows a minimum only along the Cl-O coordinate, when the Cl-O-H angle is also varied there is no minimum about the  $\text{Cl-O}\approx 2.6\text{\AA}$  and  $\text{Cl-O-H}\approx 78^\circ$  geometry). In the limits of the extrapolation of the results obtained for the gas phase complex to the results obtained for the six water cluster and the bulk system we conclude that the observed

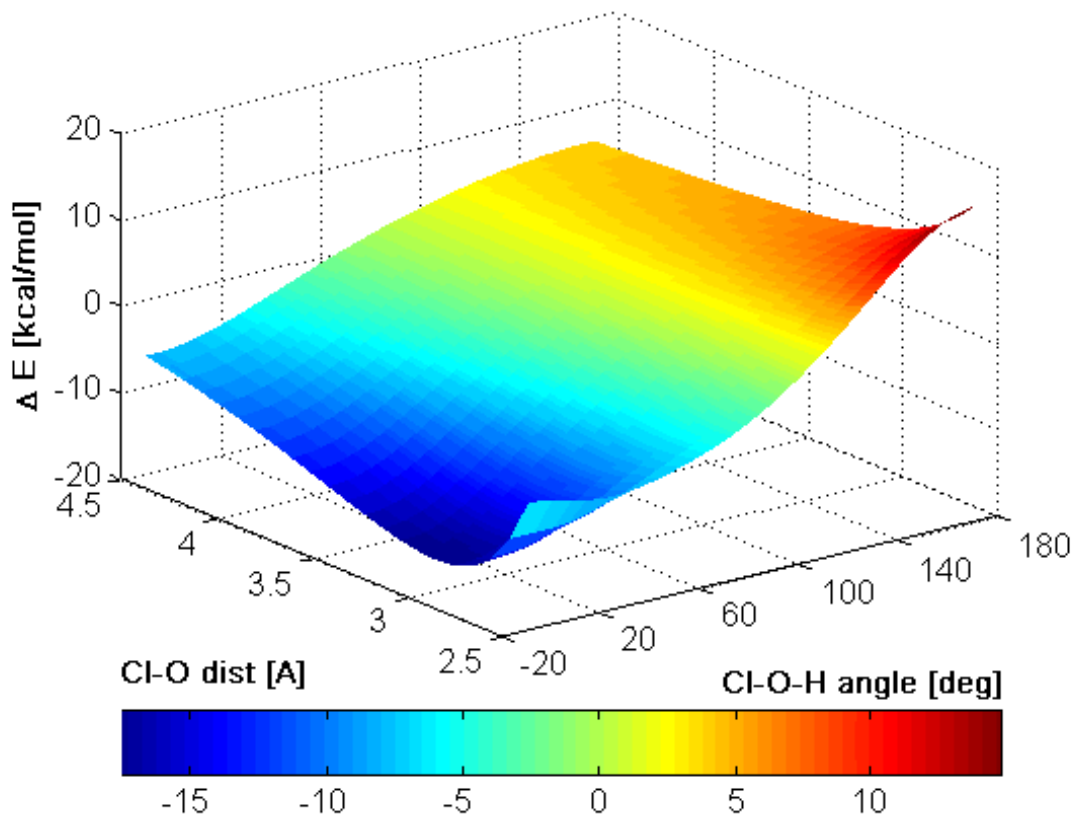


**Figure 8.** Scan of the potential energy surface of the  $\text{OHCl}^-$  complex. The O-H distance is fixed at  $1\text{\AA}$ .

covalently bonded complex in the SIE uncorrected BLYP computations represents a failure of the computational technique itself. At the same time the results obtained with the SIE corrected DFT technique show to describe the complex accurately.

## Conclusions

We have presented results from an ab initio molecular dynamics study of the chloride ion-hydroxyl radical in asymmetric and symmetric solvation environments. The complex appears to exist in two different base configurations depending on the use of a standard BLYP DFT scheme

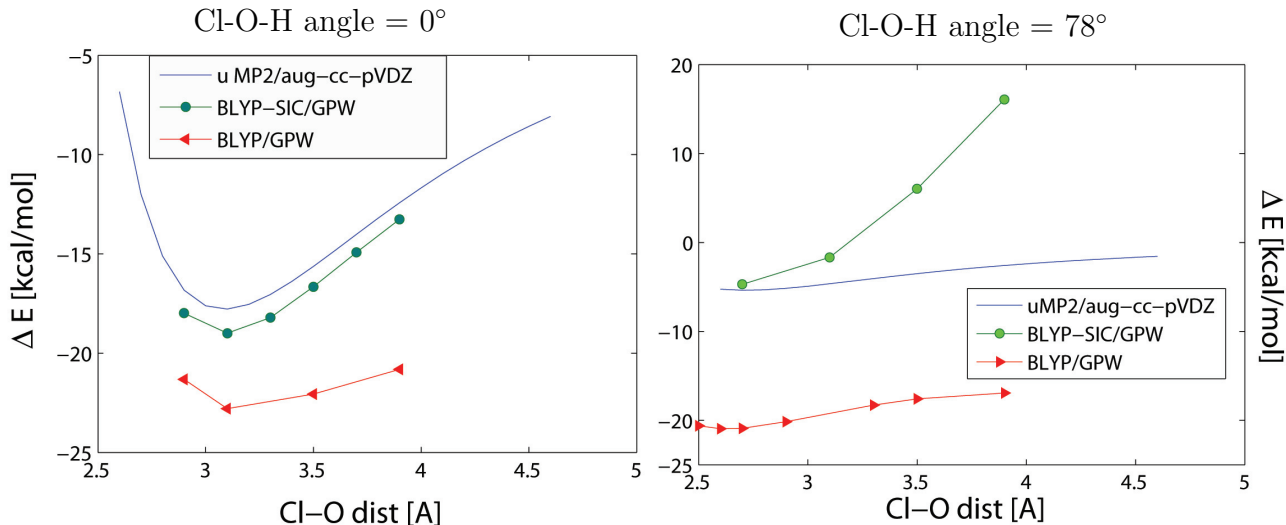


**Figure 9.** Comparison of the PES scan along  $0^\circ$  and  $78^\circ$  Cl-O-H angles.

versus a SIE-corrected BLYP DFT one. We have compared results obtained with the two DFT schemes to an uMP2/aug-cc-pVDZ scan of the ground state energy landscape of the complex in the gas phase. The absence of a local minimum in the vicinity of the geometry predicted by the uncorrected DFT results is taken as evidence of the fact that standard DFT techniques fail to capture the right geometry of open shell system such as the one under consideration due to the inherent presence of the self interaction error. On the other hand SIE-corrected BLYP results show to predict correctly the behavior of our open shell system. The SIE correction scheme that we have used has been already shown to yield results for the OH-water system in good agreement with high level ab initio computations<sup>(15)</sup>. On the point of view of the oxidation reaction of  $(\text{Cl}^-)_{\text{int}}$  to  $(\text{Cl}_2)_{\text{gas}}$  we conclude that, since no evidence of charge transfer between  $\text{Cl}^-$  and OH is observed in the cluster as well as in the bulk systems, the likely path to oxidation goes through the formation of the H-bonded  $\text{OHCl}^-$  complex and the interaction of the latter with a second  $\text{Cl}^-$ .

## Acknowledgment

This work has been supported by the AirUCI Environmental Molecular Sciences Institute under grants CHE043312 and CHE0209719 from the National Science Foundation. Part of this work was performed under the auspices of the U.S. Department of Energy by University of California LLNL under contract No. W-7405-Eng-48. Computer resources were provided by \*\*\*\*\* cluster at UCI and Livermore Computing at LLNL.

This work performed under the auspices of the U.S. Department of Energy by Lawrence Livermore National Laboratory under Contract DE-AC52-07NA27344.

## References and Notes

- (1) Jayson, G. G.; B. J. Parsons; and A. J. Swallow, *J. Chem. Soc., Faraday Trans.*, *69*, 1597–1607, 1973.
- (2) Treinin, A; E. Hayon; *J. Am. Chem. Soc.*, *97*, 1716–1721, 1975.
- (3) Sevilla, M. D.; S. Summerfield; I. Elizer; J. Rak; and M. C. R. Symons; *J. Phys. Chem. A*, *101*, 2910–2915, 1997.
- (4) Davis, M. J.; H. Koizumi; G. C. Schatz; S. E. Bradforth; and D. M. Neumark; *J. Chem. Phys.*, *101*, 4708–4721, 1994.
- (5) Spicer, C. W.; E. G. Chapman; B. J. Finlayson-Pitts; R. A. Plastridge; J. M. Hubbe; J. D. Fast; C. M. Berkowitz; *Nature*, *394*, 353–356, 1998.
- (6) Knipping, E. M.; M. J. Lakin; K. L. Foster; P. Jungwirth; D. J. Tobias; R. B. Gerber; D. Dabdub; B. J. Finlayson-Pitts; *Science*, *288*, 301–306, 2000.
- (7) Jungwirth, P.; and D. J. Tobias; *J. Phys. Chem. B*, *104*, 7702–7706, 2000.
- (8) Roeselová M.; J. Vieceli; L.X. Dang; B.C. Garrett; and D.J. Tobias; *J. Am. Chem. Soc.*, *126*, 16308-16309, 2004. For details on the computation of the interfacial concentration of OH see the article “supporting informations”.
- (9) Schulz, P.A.; R.D. Mead; P.L. Jones; W.C. Lineberger; *J. Chem. Phys.*, *77*, 1153-1165, 1982.
- (10) Trainham, R.; G.D. Fletcher; D.J. Larson; *J. Phys. B: At. Mol. Opt. Phys.*, *20*, L777-L784, 1987.

- (11) CP2K developers group, *CP2K*, 2005, <http://cp2k.berlios.de/>.
- (12) VandeVondele, J.; M. Krack; F. Mohamed; M. Parrinello; T. Chassaing and J. Hutter, *Comp. Phys. Comm.*, *167*, 103–128, 2005.
- (13) Lippert, G.; J. Hutter; and M. Parrinello; *Molec. Phys.*, *92*, 477–488, 1997.
- (14) d’Avezac, M.; M. Calandra; and F. Mauri, *Phys. Rev. B*, *71*, 205210-1–205210-5, 2005.
- (15) VandeVondele, J.; and M. Sprik, *Phys. Chem. Chem. Phys.*, *7*, 1363–1367, 2005.
- (16) Wannier, G. H.; *Phys. Rev.*, *52*, 191–197, 1937.
- (17) Marzari, N.; and D. Vanderbilt; *Phys. Rev. B*, *56*, 12847–12865, 1997.
- (18) Gaussian 98 (Revision A.1x), M. J. Frisch, G. W. Trucks, H. B. Schlegel, G. E. Scuseria, M. A. Robb, J. R. Cheeseman, V. G. Zakrzewski, J. A. Montgomery, Jr., R. E. Stratmann, J. C. Burant, S. Dapprich, J. M. Millam, A. D. Daniels, K. N. Kudin, M. C. Strain, O. Farkas, J. Tomasi, V. Barone, M. Cossi, R. Cammi, B. Mennucci, C. Pomelli, C. Adamo, S. Clifford, J. Ochterski, G. A. Petersson, P. Y. Ayala, Q. Cui, K. Morokuma, P. Salvador, J. J. Dannenberg, D. K. Malick, A. D. Rabuck, K. Raghavachari, J. B. Foresman, J. Cioslowski, J. V. Ortiz, A. G. Baboul, B. B. Stefanov, G. Liu, A. Liashenko, P. Piskorz, I. Komaromi, R. Gomperts, R. L. Martin, D. J. Fox, T. Keith, M. A. Al-Laham, C. Y. Peng, A. Nanayakkara, M. Challacombe, P. M. W. Gill, B. Johnson, W. Chen, M. W. Wong, J. L. Andres, C. Gonzalez, M. Head-Gordon, E. S. Replogle, and J. A. Pople, Gaussian, Inc., Pittsburgh PA, 2001.
- (19) Goedecker, S.; Teter, M.; Hutter, J., *Phys. Rev. B*, *54*, 1703–1710, 1996.

- (20) Becke, A. D.; *J. Chem. Phys.*, *98*, 5648–5652, 1993. Lee, C.; W. Yang; and R. G. Parr; *Phys. Rev. B*, *37*, 785–789, 1988.